O-GlcNAcylation of core components of the translation initiation machinery regulates protein synthesis

Xuexia Li[a,1], Qiang Zhu[a,1], Xiaoliu Shi[a], Yaxian Cheng[a], Xueliu Li[a], Huan Xu[a], Xiaotao Duan[b], Linda C. Hsieh-Wilson[c], Jennifer Chu[d], Jerry Pelletier[d], Maowei Ni[e], Zhiguo Zheng[e], Sihui Li[a,2], and Wen Yi[a,2]

[a]Ministry of Education Laboratory of Biosystems Homeostasis & Protection, College of Life Sciences, Zhejiang University, 310058 Hangzhou, China; [b]State Key Laboratory of Toxicology and Medical Countermeasures, Beijing Institute of Pharmacology and Toxicology, 100850 Beijing, China; [c]Division of Chemistry and Chemical Engineering, California Institute of Technology, Pasadena, CA 91125; [d]Department of Biochemistry, McGill University, Montreal, QC H3G 1Y6, Canada; and [e]Zhejiang Cancer Hospital, Zhejiang Cancer Research Institute, 310022 Hangzhou, China

Edited by Barry S. Cooperman, University of Pennsylvania, Philadelphia, PA, and accepted by Editorial Board Member Yale E. Goldman March 6, 2019 (received for review July 30, 2018)

Protein synthesis is essential for cell growth, proliferation, and survival. Protein synthesis is a tightly regulated process that involves multiple mechanisms. Deregulation of protein synthesis is considered as a key factor in the development and progression of a number of diseases, such as cancer. Here we show that the dynamic modification of proteins by O-linked β-*N*-acetyl-glucosamine (O-GlcNAcylation) regulates translation initiation by modifying core initiation factors eIF4A and eIF4G, respectively. Mechanistically, site-specific O-GlcNAcylation of eIF4A on Ser322/323 disrupts the formation of the translation initiation complex by perturbing its interaction with eIF4G. In addition, O-GlcNAcylation inhibits the duplex unwinding activity of eIF4A, leading to impaired protein synthesis, and decreased cell proliferation. In contrast, site-specific O-GlcNAcylation of eIF4G on Ser61 promotes its interaction with poly(A)-binding protein (PABP) and poly(A) mRNA. Depletion of eIF4G O-GlcNAcylation results in inhibition of protein synthesis, cell proliferation, and soft agar colony formation. The differential glycosylation of eIF4A and eIF4G appears to be regulated in the initiation complex to fine-tune protein synthesis. Our study thus expands the current understanding of protein synthesis, and adds another dimension of complexity to translational control of cellular proteins.

protein synthesis | translation initiation | glycosylation

Protein synthesis is a tightly regulated process and is essential for cell growth and proliferation. Protein synthesis contains three stages, including translation initiation, elongation, and termination. It is well accepted that protein synthesis is primarily regulated during the translation initiation stage, where ribosomal subunits are recruited to the mRNA facilitated by the eukaryotic initiation factor 4F (eIF4F) (1–3). eIF4F is a heterotrimeric complex composed of an mRNA cap-binding protein (eIF4E), a scaffolding protein (eIF4G), and an ATP-dependent RNA helicase (eIF4A). eIF4E binds to the mRNA 5′ cap structure and facilitates the recruitment of mRNA to ribosomes (4, 5). eIF4Gbridges eIF4E and eIF4A, and further stabilizes the cap-eIF4E interaction (6). eIF4A acts as a RNA helicase to remodel 5′-proximal secondary structure to facilitate 40S ribosome recruitment (7, 8).

Formation of eIF4F, one of the rate-limiting steps during initiation, is aberrantly regulated during cellular transformation and tumorigenesis (3, 9). Overexpression of eIF4E or eIF4G induces cellular transformation in different cell-based experiments (10–13). Increased signaling flux through mitogenic signaling pathways converging on mTORC1 promotes eIF4F assembly and activity. mTORC1 activation leads to phosphorylation of eIF4E-binding proteins (4EBPs) and programmed cell death 4 (PDCD4), two intrinsic inhibitory binding partners of eIF4E and eIF4A, respectively, thus liberating eIF4E and eIF4A to engage in the binding of eIF4G (14, 15). Ras pathway signaling through Erk stimulates the MNK kinases to phosphorylate eIF4E at serine 209. This phosphorylation event stimulates translation of a subset of mRNAs important for cell growth, proliferation, and metastasis, leading to enhanced cellular transformation both in cultured cells and in vivo (16). Disruption of eIF4F activity or assembly by either genetic approaches or small-molecule inhibitors potently impairs tumor formation in mouse models (17). Despite these studies, the molecular mechanisms that regulate eIF4F activity/assembly have not been fully defined and are required to improve our current understanding of the relationship between translation regulation and cellular transformation.

O-linked β-*N*-acetylglucosamine (O-GlcNAc) is a prevalent posttranslational modification of nuclear and cytosolic proteins (18). Cycling of O-GlcNAc on proteins is controlled by the action of a set of enzymes in cells. O-GlcNAc transferase (OGT) catalyzes the addition of GlcNAc to proteins, while O-GlcNAc hydrolase (OGA) is responsible for removal of the GlcNAc moiety. Research has identified hundreds of intracellular proteins containing the modification. Increasing evidence has shown that O-GlcNAcylation regulates various important biological processes, including transcription, stem-cell differentiation, signal transduction, cell cycle progression, and metabolic reprogramming (19, 20). Recently, a few studies have reported that proteins involved in the translation process and ribosomal biogenesis are O-GlcNAcylated, raising an intriguing possibility

Significance

Protein synthesis is essential for cell growth, proliferation, and survival. Deregulation of protein synthesis is an important feature in many diseases. However, how protein synthesis is regulated under physiological and pathological conditions still remains poorly understood. In this study, we report an unknown mechanism for the regulation of protein synthesis in cells. We demonstrate that two important translation initiation factors, namely eIF4A and eIF4G, are modified by a single sugar N-acetylglucosamine. Detailed analyses show that this modification influences the interaction and function of these two proteins, and regulates protein synthesis at the initiation stage. This finding expands the current understanding of protein synthesis and adds a dimension of complexity to translational control of cellular proteins in cells.

Author contributions: W.Y. designed research; Xuexia Li, Q.Z., X.S., Y.C., Xueliu Li, H.X., and X.D. performed research; X.D., L.C.H.-W., J.C., J.P., M.N., and Z.Z. contributed reagents/analytic tools; Xuexia Li, Q.Z., X.S., Y.C., Xueliu Li, X.D., J.C., J.P., S.L., and W.Y. analyzed data; and S.L. and W.Y. wrote the paper.

The authors declare no conflict of interest.

This article is a PNAS Direct Submission. B.S.C. is a guest editor invited by the Editorial Board.

[1]Xuexia Li and Q.Z. contributed equally to this work.

[2]To whom correspondence may be addressed. Email: lisihui@zju.edu.cn or wyi@zju.edu.cn.

This article contains supporting information online at www.pnas.org/lookup/suppl/doi:10.1073/pnas.1813026116/-/DCSupplemental.

Published online April 2, 2019.

that O-GlcNAcylation regulates protein synthesis (21–23). For example, Datta et al. (24, 25) showed that O-GlcNAcylation of p67 protected the eukaryotic initiation factor 2α (eIF2α) from phosphorylation by eIF2 kinase, leading to enhanced protein synthesis. Duan et al. (22) demonstrated that O-GlcNAcylation of a ribosomal protein RACK1 induced protein synthesis and was required for tumorigenesis in liver cancer. Despite these elegant studies, the understanding of the mechanistic link between O-GlcNAcylation and protein synthesis still remains incomplete.

Here, we demonstrate that O-GlcNAcylation regulates protein synthesis by modifying the core translation factors eIF4A and eIF4G, respectively. Mechanistically, site-specific O-GlcNAcylation of eIF4A disrupts eIF4F assembly by perturbing its interaction with eIF4G. In addition, O-GlcNAcylation inhibits the duplex unwinding activity of eIF4A. Collectively, eIF4A glycosylation impaired protein synthesis, and reduced cell proliferation. In contrast, site-specific O-GlcNAcylation of eIF4G at its N terminus promotes its interaction with poly(A)-binding protein (PABP) and poly(A) RNA, with no obvious effect on the interaction with eIF4A or eIF4E. Depletion of eIF4G O-GlcNAcylation results in inhibition of protein synthesis and cell proliferation. In addition, the differential glycosylation of eIF4A and eIF4G appears to be regulated in the eIF4F complex to fine tune protein synthesis. Thus, our study reveals a molecular mechanism for regulating protein synthesis in cells.

Results

Core Components of the Translation Initiation Complex Are Modified by O-GlcNAc. To investigate whether OGT physically associates with the translation initiation complex eIF4F in cells, we performed pull-down assays using m^7GDP affinity beads. Consistent with previous studies, eIF4F was efficiently isolated from 293T cell lysates (Fig. 1*A*) (26). OGT was readily detected in the pull-down mixture, indicating that OGT was associated with the eIF4F (Fig. 1*A*). Next we determined which protein components in the eIF4F were O-GlcNAcylated using a well-established chemoenzymatic labeling method (*SI Appendix*, Fig. S1) (23). We enzymatically labeled O-GlcNAcylated proteins in 293T cell lysates with an azido-*N*-acetylgalactosamine sugar (GalNAz). Labeled proteins were then biotinylated via Cu(I)-mediated [3+2] azide-alkyne cycloaddition chemistry and captured on streptavidin-agarose beads. Subsequent elution fractions from the beads were immunoblotted with specific antibodies against eIF4A, eIF4E, and eIF4G, respectively. Strong signals were readily detected with eIF4A and eIF4G antibodies, but not with the eIF4E antibody, suggesting that eIF4A and eIF4G were modified by O-GlcNAc (Fig. 1*B*). This is consistent with our previous proteomic studies in which eIF4A and eIF4G were identified as putative O-GlcNAcylated proteins (27). Quantification of the glycosylated protein fractions versus total proteins yielded an estimated basal level of glycosylation stoichiometries of 15 ± 5% and 7 ± 3% for eIF4A and eIF4G, respectively. Studies have shown that two other critical translation initiation factors, eIF4B and eIF4H, are strongly associated with the eIF4F complex during translation initiation (28). Therefore, we tested whether eIF4B and eIF4H were O-GlcNAcylated in cells. Results showed a weak signal for eIF4B, and no detectable signal for eIF4H, suggesting that eIF4B was weakly modified by O-GlcNAc, while eIF4H did not possess O-GlcNAcylation (Fig. 1*B*). Since OGT is physically associated with the eIF4F, it would preferentially modify eIF4A and eIF4G as subunits of the complex. As expected, in the fraction pulled down with m^7GDP beads eIF4A and eIF4G displayed higher level of glycosylation compared with eIF4A and eIF4G from the cell lysate fraction (Fig. 1*C*). In mammalian cells, both eIF4A and eIF4G have two major isoforms, namely eIF4AI, eIF4AII, eIF4GI, and eIF4GII, respectively (29, 30). Previous studies have demonstrated that eIF4AI and eIF4GI are expressed more abundantly than the other isoforms in cells (31). Using isoform-specific siRNAs, we demonstrated that depletion of isoform eIF4AI or eIF4GI strongly inhibited cell proliferation, while depletion of isoform eIF4AII or eIF4GII had a very modest effect on cell proliferation compared with the parental cells (*SI Appendix*, Fig. S2), suggesting that isoforms eIF4AI and eIF4GI are more functionally important. Thus, we focused on isoforms eIF4AI and eIF4GI in the following studies.

To investigate whether O-GlcNAcylation of eIF4AI and eIF4GI is dynamically regulated in cells, we subjected cells to different treatments and analyzed the glycosylation levels. Overexpression of OGT increased, while OGT inhibition decreased O-GlcNAcylation on both eIF4AI and eIF4GI proteins (Fig. 1*D*). Consistently, OGA overexpression decreased, while OGA inhibition increased O-GlcNAcylation levels (Fig. 1*D*). Varying concentrations of the two major nutrients (glucose and glutamine) in the culture medium resulted in altered glycosylation levels (Fig. 1*D*). Thus, O-GlcNAcylation of eIF4AI and eIF4GI is dynamically regulated in cells.

We further examined whether O-GlcNAcylation of eIF4AI and eIF4GI occurs across different malignant and noncancerous cells. Glycosylation of eIF4AI and eIF4GI was detected in a wide range of malignant cell lines, to varied degrees (Fig. 1 *E* and *F*). Notably, the glycosylation level of eIF4AI in noncancerous cells was significantly higher than that in malignant cells of the same cell type, as shown in ovarian, stomach, and liver cell lines (Fig. 1*E*). In contrast, the glycosylation level of eIF4GI in noncancerous cells was significantly lower than that in malignant cells of the same cell type, as shown in ovarian, stomach, and breast cell lines (Fig. 1*F*). It appears that cancer cells down-regulate eIF4AI glycosylation, but up-regulate eIF4GI glycosylation.

To correlate eIF4A and eIF4G glycosylation with clinical disease progression, we examined human tumor tissue samples and normal tissue samples (*SI Appendix*, Fig. S3). Consistent with the results observed from the cell lines, eIF4A O-GlcNAcylation levels were decreased in ovarian tumor tissues compared with that in normal tissues. On the other hand, the majority of breast tumor tissues exhibited relatively higher levels of eIF4G glycosylation compared with normal tissues. The differences in glycosylation patterns observed in both cell lines and tissues between eIF4AI and eIF4GI suggest a differential role for O-GlcNAcylation in regulating their biological functions in vivo.

O-GlcNAcylation of eIF4AI Disrupts Assembly of the eIF4F. To investigate the role of O-GlcNAcylation on eIF4AI, we first determined its glycosylation site(s). Flag-tagged eIF4AIproteins were expressed in 293T cells. After immunoprecipitation of Flag-tagged eIF4AI and in-gel trypsin digestion, peptides were subjected to mass spectrometry analysis. Glycosylation sites were mapped to serine 322 and serine 323 (*SI Appendix*, Fig. S4). Single site mutations (S322A/Y or S323A/Y) only modestly reduced the level of glycosylation compared with the wild type (Fig. 2*A*). Double site mutations (S322/S323A or S322/S323Y) nearly abolished the glycosylation signals, indicating that Ser322 and Ser323 are the major glycosylation sites on eIF4AI (Fig. 2*A*).

Sequence comparison analysis showed that Ser322 and Ser323 were conserved residues in homolog eIF4A proteins across different species, indicating a possible functional role for these residues (Fig. 2*B*). Three-dimensional structures have been determined for a few eIF4A proteins from different species (32). Structural analysis revealed that the glycosylation sites resided in a loop structure connecting an alpha helix and a beta sheet (Fig. 2*C*). Notably, a protein complex structure determined with yeast eIF4AI and eIF4GI revealed that the conserved sequence (SGSSR) containing the glycosylation sites resided at the interface where eIF4AI and eIF4GI interacted (Fig. 2*C*) (33). Although the internal serine residues in the SGSSR corresponding to the glycosylation sites did not form any direct hydrogen bonds with residues in eIF4GI, a bulky GlcNAc modification would very likely cause

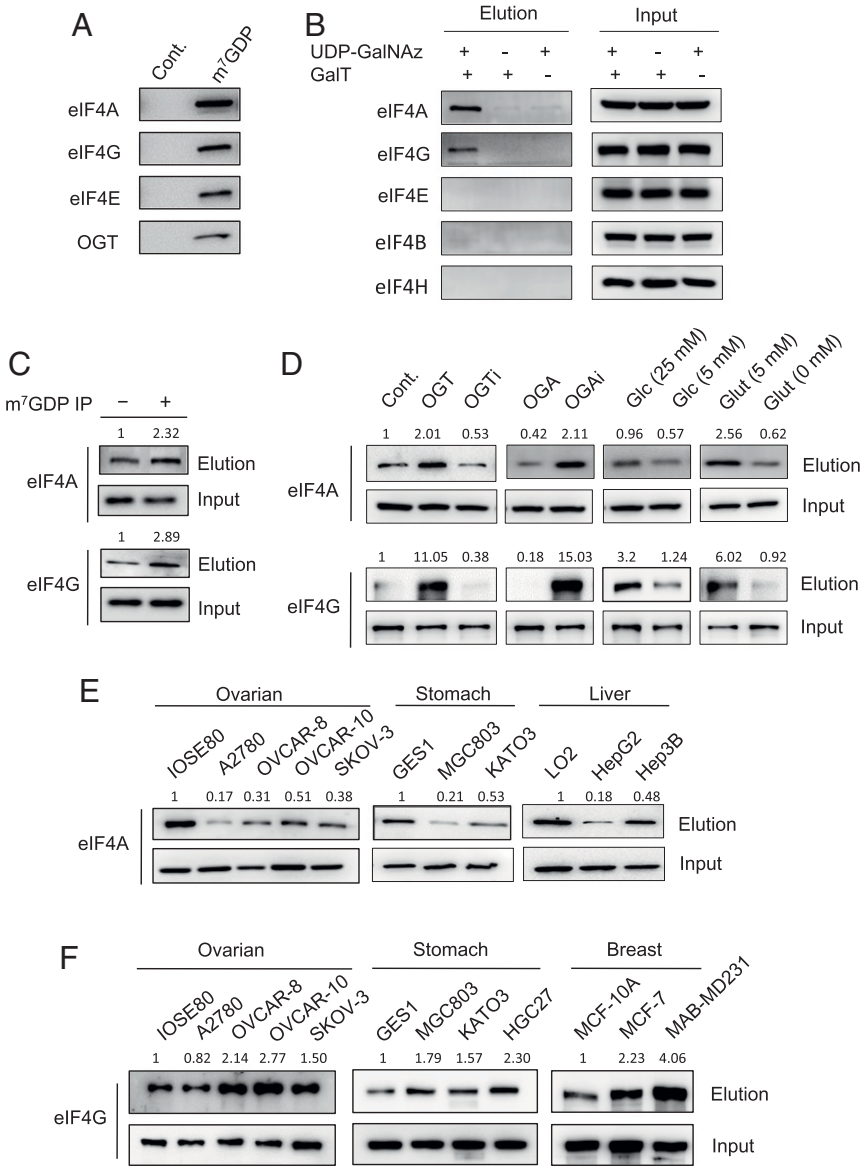

Fig. 1. Core components of the translation initiation complex are modified by O-GlcNAc. (*A*) OGT associates with the translation initiation complex eIF4F in cells. The eIF4F complex was isolated from 293T cell lysates using m^7GDP affinity beads. After elution from the beads, Western blot analysis was performed with antibodies against eIF4A, eIF4E, eIF4G, or OGT. The control experiment (Cont.) was performed similarly with protein G agarose beads. (*B*) Key components (eIF4A and eIF4G) of the translation initiation complex are modified by O-GlcNAc. The isolation and detection of specific O-GlcNAcylated proteins in cell lysates are described in *SI Appendix*. As input, 10% of total protein was loaded. (*C*) O-GlcNAcylation preferentially occurs on eIF4AI and eIF4GI as subunits of the eIF4F. The eIF4F was pulled down using m^7GDP beads, and the glycosylation of eIF4AI and eIF4GI was analyzed. (*D*) O-GlcNAcylation of eIF4AI and eIF4GI is dynamically regulated in cells. HEK293T cells were subjected to different treatments (Cont., Control; Glc, Glucose; Glut, Glutamine; OGA, OGA overexpression; OGAi, OGA inhibition with ThiaMet G; OGT, OGT overexpression; OGTi: OGT inhibition with ST045849), and the O-GlcNAcylation levels of eIF4AI and eIF4GI were analyzed. Quantification of protein levels was indicated. As input, 8% of total protein was loaded. (*E*) Glycosylation of eIF4AI was up-regulated in noncancerous cells (IOSE80, GES1, and LO2) compared with malignant cells, as shown in ovarian, stomach, and liver cell lines. Quantification of protein levels was indicated. (*F*) Glycosylation of eIF4GI was down-regulated in noncancerous cells (IOSE80, GES1, and MCF-10A) compared with malignant cells, as shown in ovarian, stomach, and breast cell lines. Quantification of protein levels was indicated.

substantial perturbations in the protein–protein interaction. To verify this on human eIF4AI, we generated a S322/S323A mutant (a mimetic of deglycosylation) and a S322/S323Y mutant (a mimetic of bulky glycosylation). A tyrosine residue has been demonstrated in a recent report to be a proper mimetic of O-GlcNAcylation due to its bulky size (34). Flag-tagged eIF4AI WT or mutants were stably transfected in 293T cells. Immunoprecipitation was carried out using anti-Flag M2 beads, and further immunoblotted with an antibody against eIF4GI. Results showed that comparable amounts of eIF4GI were pulled down in WT and S322/S323A expressing cells, while significantly less amounts of eIF4GI were detected in S322/S323Y expressing cells, consistent with the prediction that O-GlcNAcylation disrupted the eIF4AI and eIF4GI interaction (Fig. 2*D*). As a further verification, we increased O-GlcNAcylation in the WT eIF4AI expressing cells by Thiamet G (TMG) treatment (inhibition of OGA) or OGT overexpression, and immunoblotted eIF4GI after M2 bead pull-down. We observed that increasing eIF4AI glycosylation led to decreased amounts of eIF4GI during the pull-down, suggesting a loss of interaction between eIF4AI and eIF4GI (Fig. 2*E*). TMG treatment and OGT overexpression

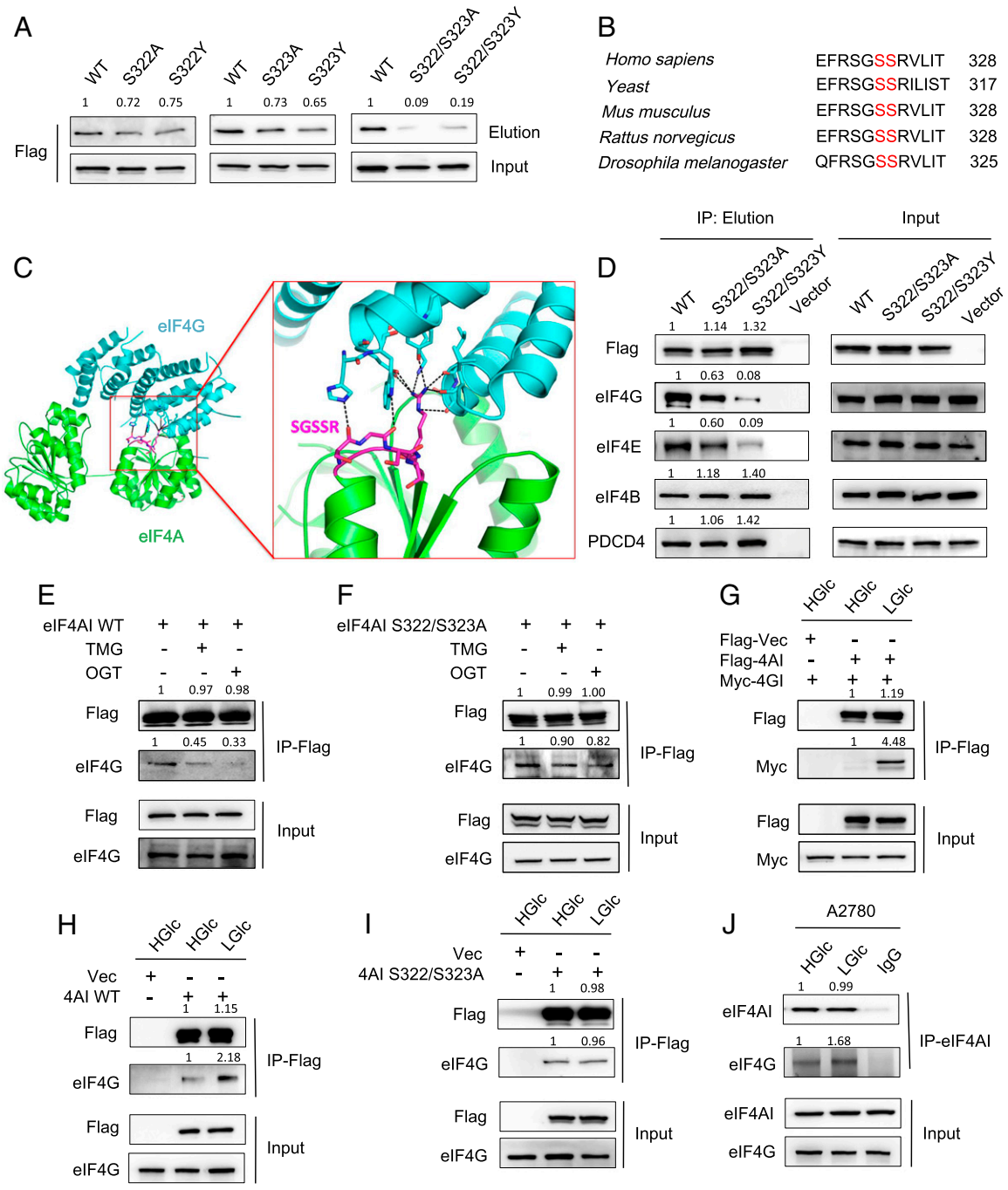

Fig. 2. O-GlcNAcylation of eIF4AI disrupts assembly of the eIF4F. (*A*) S322 and S323 are the major glycosylation sites of eIF4AI. Site-specific mutations were generated: single mutants (S322A, S322Y, S323A, S323Y) and double mutants (S322/S323A, S322/S323Y). Glycosylation levels of these mutants were analyzed using the chemoenzymatic method and compared with the WT protein. Quantification of protein levels was indicated. As input, 10% of total protein was loaded. (*B*) The glycosylation sites of eIF4AI are conserved across different species. Human (NP_001191439.1), *Saccharomyces cerevisiae* (NP_012985.3), *Musmusculus* (NP_001152847.1), *Rattusnorvegicus* (NP_001093628.1), *Drosophila melanogaster* (NP_001245907.1). (*C*) The glycosylation sites of eIF4AI reside at the interaction interface between eIF4AI and eIF4GI. The crystal structure of the yeast eIF4A-eIF4G complex was obtained from the Protein Data Bank databank (2VSO). (*D*) The effect of eIF4AI glycosylation site mutations on protein–protein interactions. Flag-tagged WT, S322/323A, or S322/323Y eIF4AI was stably expressed in 293T cells. Immunoprecipitation was carried out using anti-Flag M2 beads, and the pull-down complex was immunoblotted with the indicated antibodies. Quantification of protein levels was indicated. As input, 5% of total protein was loaded. (*E* and *F*) Increasing eIF4AI glycosylation reduces the interaction with eIF4GI. HEK293T cells expressing Flag-tagged WT or S322/323A eIF4AI were subjected to TMG treatment or OGT expression. Immunoprecipitation was carried out using anti-Flag M2 beads, and the eluent was immunoblotted with eIF4GI antibodies. Quantification of protein levels was indicated. As input, 5% of total protein was loaded. (*G–I*) The interaction of eIF4AI and eIF4GI is increased in the presence of low glucose concentration. Flag-tagged WT eIF4AI, S322/323A eIF4AI, or Myc-tagged eIF4GI was individually or coexpressed in 293T cells in the presence of high- (HGlc, 25 mM) or low (LGlc, 5 mM) glucose concentrations. Immunoprecipitation was carried out using anti-Flag M2 beads, and the eluent was immunoblotted with the indicated antibodies. Quantification of protein levels was indicated. As input, 5% of total protein was loaded. (*J*) The interaction of endogenous eIF4AI and eIF4GI is increased in the presence of low glucose concentration. Ovarian cancer cell line A2780 was cultured in the presence of high- (HGlc, 25 mM) or low (LGlc, 5 mM) glucose concentrations. Immunoprecipitation was carried out using an eIF4AI antibody, and the eluent was immunoblotted with an eIF4GI antibody. Quantification of protein levels was indicated. As input, 10% of total protein was loaded.

induced eIF4AI glycosylation levels by about 3.1- and 4.3-fold, respectively (*SI Appendix*, Fig. S5*A*). Given the basal glycosylation level of eIF4AI around 15%, the glycosylation levels upon TMG treatment or OGT overexpression are estimated to be 45 and 64%, respectively. In contrast, in the S322/S323A mutant expressing cells, TMG treatment or OGT overexpression appeared to have no effect on the detection signals of eIF4GI (Fig. 2*F*). We further cultured cells in different concentrations of glucose, and consistently observed that in WT but not S322/S323A mutant expressing cells, a low glucose level enhanced the interaction, while a high glucose level reduced the interaction (Fig. 2 *G*–*I* and *SI Appendix*, Fig. S5*B*). To verify the effect of O-GlcNAcylation on endogenous proteins, ovarian cancer cell line A2780 was cultured in the presence of 5- or 25 mM glucose. The interaction between eIF4AI and eIF4G was higher in 5 mM glucose concentration (Fig. 2*J*). Collectively, our results showed that O-GlcNAcylation of eIF4AI inhibited its interaction with eIF4GI.

Although eIF4E does not directly interact with eIF4AI, it is known to associate with eIF4AI in the complex through an interaction with eIF4GI. Consistently, the association of eIF4E with eIF4AI followed the same trend as that observed between eIF4AI and eIF4GI (Fig. 2*D*). O-GlcNAcylation on eIF4AI did not appear to affect its interaction with eIF4B or PDCD4, an intrinsic inhibitor of eIF4AI (Fig. 2*D*).

O-GlcNAcylation of eIF4AI Inhibits Its Helicase Activity and Impairs Protein Synthesis and Cell Proliferation. To understand the impact of O-GlcNAcylation on eIF4AI function, we investigated the duplex unwinding activity (helicase activity) of different eIF4AI variants. Similar helicase activities were observed with WT and S322/S323A mutant proteins (Fig. 3*A*). However, the S322/S323Y mutant showed a significantly reduced helicase activity (Fig. 3*A*). To further verify the effect of O-GlcNAcylation, we obtained bacterially expressed His-tagged eIF4AI as a nonglycosylated protein, and purified 293T-expressed Flag-tagged eIF4AI (with TMG treatment to enhance glycosylation) as an O-GlcNAcylated protein (*SI Appendix*, Fig. S6). We then compared the duplex unwinding activity between these two forms of proteins. Consistent with the mutagenesis studies, O-GlcNAcylated eIF4AI exhibited lower duplex unwinding activity compared with the nonglycosylated counterpart (Fig. 3*B*).

As O-GlcNAcylation of eIF4AI appears to disrupt the assembly of eIF4F and inhibit the helicase activity, we speculated that cellular protein synthesis would be affected. We first analyzed the in vitro translation activity using the rabbit reticulocyte lysate system. Addition of the S322/S323Y mutant eIF4AI inhibited the translation efficiency in a dose-dependent manner, while addition of the S322/S323A mutant did not show detectable inhibition (*SI Appendix*, Fig. S7*A*). Consistently, addition of the TMG-treated

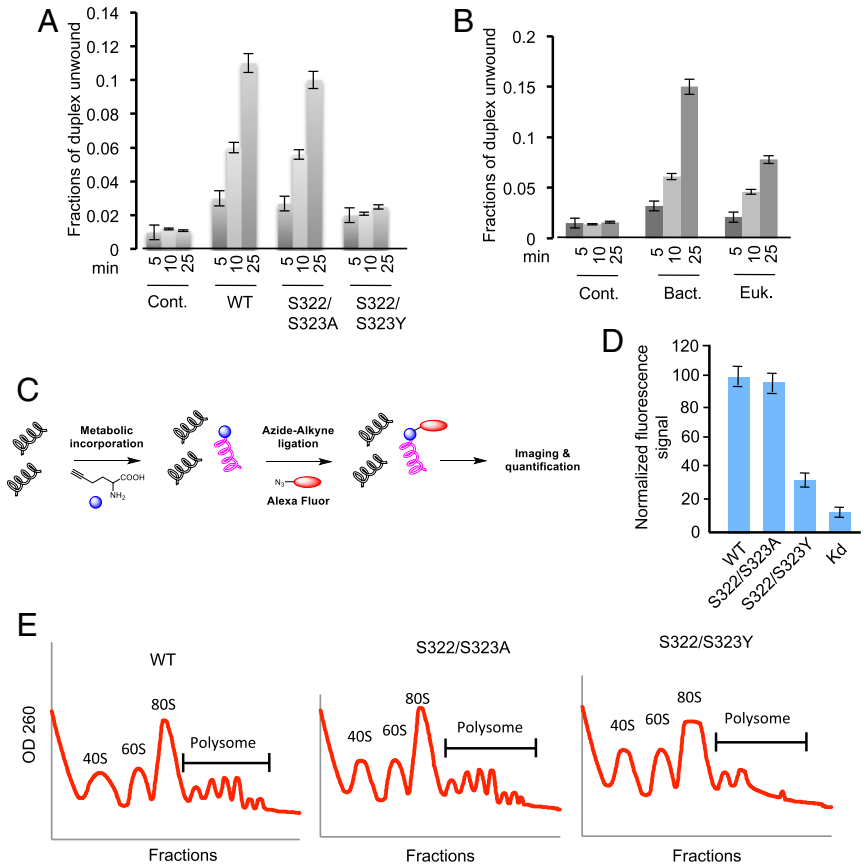

Fig. 3. O-GlcNAcylation of eIF4AI negatively regulates its activity and impairs protein synthesis. (*A*) Determination of the duplex unwinding activity of WT, S322/S323A, and S322/S323Y eIF4AI, as described in *SI Appendix*. A control experiment was performed in the absence of eIF4AI (Cont.). (*B*) Comparison of the duplex unwinding activity between bacterially expressed (Bact.) eIF4AI and 293T-expressed (Euk.) eIF4AI. Coomassie Brilliant Blue staining was performed to verify protein expression. A control experiment was performed in the absence of eIF4AI (Cont.). (*C*) Strategy for determination of nascent protein synthesis in 293T cells stably expressing WT, S322/S323A, or S322/S323Y eIF4AI. Cells were metabolically labeled with HPG, a synthetic analog of methionine containing an alkyne functionality, and the synthesized proteins were detected using a bioorthogonal chemical ligation with azido-containing Alexa Fluor 488. Fluorescence signal intensity was normalized with respect to the cell numbers and represented the amount of synthesized protein pools. (*D*) Quantification of nascent protein synthesis rates in 293T cells stably expressing WT, S322/S323A, or S322/S323Y eIF4AI. A control experiment was performed using cells with depletion of eIF4AI (K_d). (*E*) Polysome profiling analysis of 293T cells stably expressing WT, S322/S323A, or S322/S323Y eIF4AI.

eIF4AI reduced the translation activity compared with addition of nontreated eIF4AI (*SI Appendix*, Fig. S7*B*). Thus, glycosylation of eIF4AI inhibited in vitro translation. To determine the effect on protein synthesis in vivo, we further analyzed the rate of nascent protein synthesis in 293T cells stably expressing WT and mutant eIF4AI. Cells were metabolically labeled with L-homopropargylglycine (HPG), a synthetic analog of methionine containing an alkyne functionality, and the synthesized proteins were detected using a bioorthogonal chemical ligation with azido-containing Alexa Fluor 488 (Fig. 3*C*) (35). Fluorescent signal intensity was normalized with respect to cell numbers and represented the amount of synthesized protein pools. In agreement with the results obtained from the in vitro translation system, cells expressing the WT or S322/S323A mutant eIF4AI displayed similar fluorescent signal intensity, while cells expressing the S322/S323Y mutant displayed markedly reduced signal intensity (Fig. 3*D*). As another confirmation, we performed the traditional [^{35}S]-methionine metabolic incorporation assay (*SI Appendix*, Fig. S8). Thus, O-GlcNAcylation of eIF4AI appears to impair translation both in vitro and in vivo. In addition, polysome profiling analysis showed that the S322/S323Y mutant expressing cells displayed reduced amounts of polysomes compared with the WT or S322/S323A mutant expressing cells (Fig. 3*E*), suggesting ineffective translation in the S322/S323Y mutant expressing cells.

We further validated the function of eIF4AI glycosylation using A2780 ovarian cancer cells that stably expressed Flag-tagged WT or mutant eIF4AI with simultaneous depletion of endogenous eIF4AI (*SI Appendix*, Fig. S9*A*). Consistent with the effect on nascent protein synthesis, cells expressing the WT or S322/S323A mutant showed comparable rates of cell proliferation, while cells expressing the S322/S323Y mutant showed markedly reduced cell proliferation rate (*SI Appendix*, Fig. S9*B*). Soft agar colony formation assays also demonstrated that cells expressing the S322/S323Y mutant showed significantly reduced ability to form colonies compared with cells expressing the WT or S322/S323A mutant (*SI Appendix*, Fig. S9*C*). Collectively, O-GlcNAcylation of eIF4AI inhibits its helicase activity, and impairs protein synthesis and cell proliferation.

O-GlcNAcylation of eIF4GI Promotes Assembly of mRNP During the Initiation. To investigate the role of O-GlcNAcylation on eIF4GI, we determined its glycosylation site(s). In our previous study, using mass spectrometry we mapped the glycosylation sites to a peptide 56-AQPPSSAASR-65 (27). Mutation of a single residue, Ser60 or Ser64, to alanine only modestly reduced eIF4GI glycosylation in cells, while mutation of Ser61 to alanine markedly reduced eIF4GI glycosylation (Fig. 4*A*). Furthermore, simultaneous mutations of all three serine residues to alanine led to a comparable reduction of glycosylation signals compared with the S61A mutant (Fig. 4*A*). These results suggest that Ser61 is the major glycosylation site in eIF4GI. Thus, the S61A mutant was used in subsequent studies to analyze the role of glycosylation on eIF4GI.

We investigated whether glycosylation of eIF4GI affected its interaction with known binding proteins. Flag-tagged eIF4GI WT or S61A mutant was stably expressed in 293T cells. Immunoprecipitation was carried out using anti-Flag M2 beads, and the pull-down mixture was further immunoblotted with antibodies against eIF4AI or eIF4E. We observed that comparable amounts of eIF4AI and eIF4E were pulled down in WT and mutant eIF4GI expressing cells, indicating that O-GlcNAcylation on eIF4GI did not affect its interaction with these subunits (Fig. 4*B*). Furthermore, cellular treatment with TMG had no obvious effect on the detection signals of eIF4AI or eIF4E. Previous studies have found that eIF4E interacts with the N-terminal domain and eIF4AI interacts with the middle and C-terminal domain of eIF4GI, quite remote from its O-GlcNAcylation sites, which are located near the N terminus (36). These observations lend support to the notion that unlike eIF4AI, eIF4GI glycosylation does not seem to interfere with the assembly of eIF4F.

In eukaryotes, the association of PABP and eIF4GI is critical for efficient mRNA translation. Previous studies have mapped their interaction site to the N terminus of eIF4GI (29, 37). Thus, we wanted to investigate whether O-GlcNAcylation might affect the interaction between eIF4GI and PABP. We found that significantly more PABP was pulled down in Flag-eIF4GI expressing cells treated with TMG compared with cells without TMG treatment, suggesting that increasing O-GlcNAcylation might enhance the interaction between eIF4GI and PABP (Fig. 4*B*). Expectedly, in the eIF4GI S61A mutant expressing cells, a markedly reduced amount of PABP was pulled down compared with the WT expressing cells. Treatment of the mutant expressing cells with TMG did not have any obvious effect on the PABP signal (Fig. 4*B*).

To verify further the interaction between eIF4GI and PABP, Myc-tagged PABP was generated and cotransfected in 293T cells with Flag-tagged eIF4GI. Significantly lower amounts of PABP were pulled down in the eIF4GI S61A mutant expressing cells with anti-Flag antibodies compared with the WT expressing cells, consistent with the data shown above (Fig. 4*C*). Reversal pull-down experiments using anti-Myc antibodies also showed that lower amounts of eIF4GI S61A were coimmunoprecipitated compared with eIF4GI WT (*SI Appendix*, Fig. S10). To investigate whether the O-GlcNAcylation effect on eIF4GI/PABP interaction occurs with endogenous proteins, we cultured 293T cells in the presence of low- (5 mM) or high (25 mM) concentrations of glucose, carried out immunoprecipitation using anti-eIF4GI antibodies, and immunoblotted with anti-PABP antibodies. Consistently, significantly more PABP was detected in cells grown under high glucose concentrations (Fig. 4*D*). Similar experiments were also carried out using the breast cancer cell line MCF-7, in which a similar result was obtained (Fig. 4*E*). Taken together, O-GlcNAcylation of eIF4GI enhances its interaction with PABP in cells.

Several lines of evidence have demonstrated that the eIF4GI/PABP interaction is important for the stabilization of eIF4GI binding to mRNA during translation initiation (38). Indeed, one of the RNA binding domains in eIF4GI has been mapped to the extreme N terminus of eIF4GI (amino acids 1–82), which includes the O-GlcNAcylation sites (39). Thus, we speculated that O-GlcNAcylation of eIF4GI is important for the interaction with mRNA. To test this hypothesis, we generated a bacterially expressed, recombinant GST fusion protein containing the N-terminal aa 2–300 of WT eIF4GI and the corresponding S61Aand S61Y mutants. We then analyzed the effects on RNA-binding activity by measuring the increase in fluorescence anisotropy of fluorescently labeled RNA poly(A) 50-mer upon binding to eIF4GI WT and mutant proteins. In addition, eIF4GI protein lacking the N-terminal RNA binding domain (aa 1–82) was included as a negative control. The results showed that the dissociation constant (K_d) for the WT eIF4GI fusion protein was 0.41 μM, fairly similar to that reported before (37). The S61Y mutant protein showed a slight increase in binding affinity, with a K_d of 0.32 μM. In contrast, the S61A mutant protein showed a nearly sixfold reduction in binding affinity, with a K_d of 2.38 μM. The negative control completely lacked the ability to bind RNA as expected (Fig. 4*F*). Thus, these results appear to suggest that O-GlcNAcylation of eIF4GI may promote the assembly of mRNP by enhancing the interaction with PABP and the binding of RNA to the initiation complex.

To investigate the function of eIF4GI O-GlcNAcylation in cells, we generated eIF4GI S61A knock-in MCF-7 cell lines using CRISPR-Cas9 gene editing technology. We also generated a mutant cell line by knocking out the splicing isoforms containing the glycosylation sites to serve as a positive control (*SI Appendix*, Fig. S11). We verified that O-GlcNAcylation levels of eIF4GI in these two mutant cell lines were substantially decreased compared with the parental cells (Fig. 5*A*). Immunoprecipitation with anti-eIF4GI

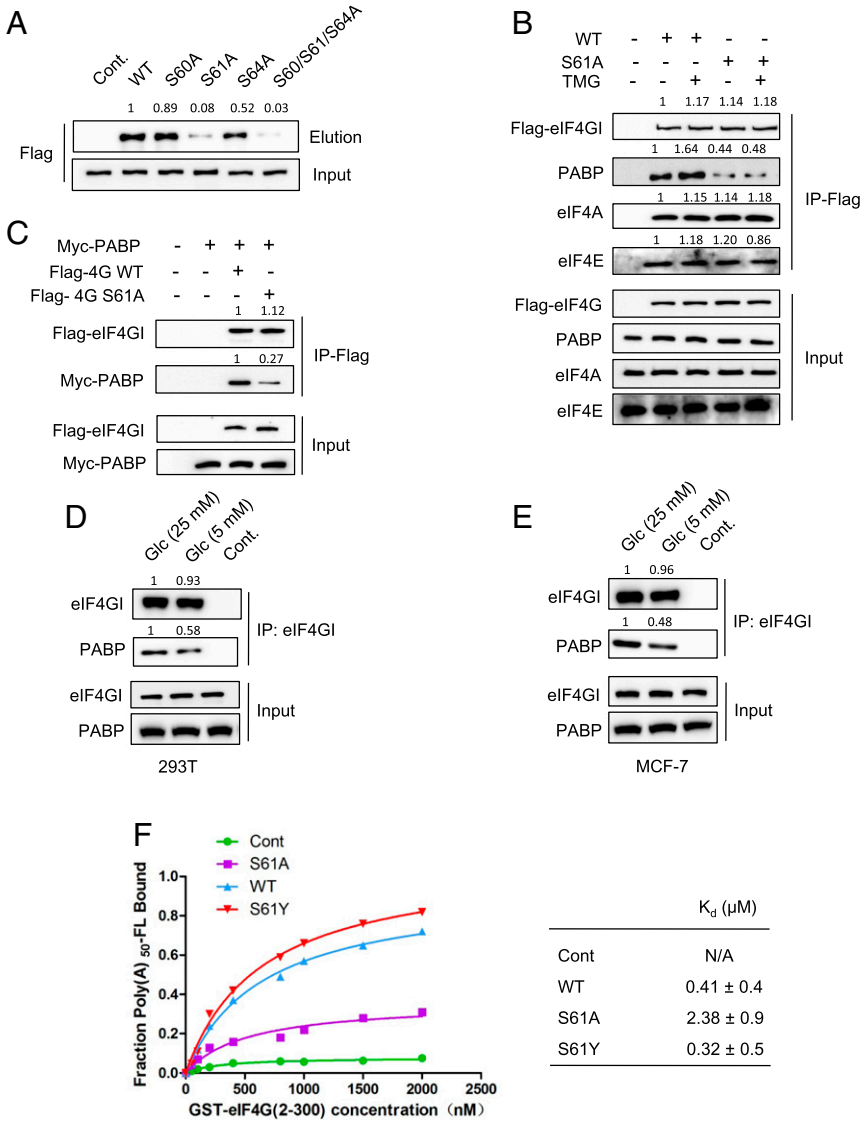

	K_d (μM)
Cont	N/A
WT	0.41 ± 0.4
S61A	2.38 ± 0.9
S61Y	0.32 ± 0.5

Fig. 4. O-GlcNAcylation of eIF4GI promotes assembly of mRNP during translation initiation. (*A*) S61 is the major glycosylation site on eIF4GI. Single- (S60A, S61A, and S64A) and triple (S60/61/64A) mutations in eIF4GI were generated. Glycosylation levels of WT and mutant eIF4GI were analyzed by the chemoenzymatic method as described above. Quantification of protein levels was indicated. As input, 8% of total protein was loaded. (*B* and *C*) S61 glycosylation of eIF4GI enhances its interaction with PABP. Flag-tagged WT, S61A eIF4GI, or Myc-tagged PABP was individually or coexpressed in 293T cells in the presence or absence of TMG. Immunoprecipitation was carried out using anti-Flag M2 beads, and the eluent was immunoblotted with the indicated antibodies. Quantification of protein levels was indicated. As input, 5% of total protein was loaded. (*D* and *E*) The interaction of endogenous eIF4GI and PABP is increased in the presence of high glucose concentration in both 293T cells (*D*) and MCF-7 cells (*E*). Quantification of protein levels was indicated. As input, 5% of total protein was loaded. (*F*) eIF4GI glycosylation promotes the interaction with poly(A) mRNA. RNA-binding activity was measured by the increase in fluorescence anisotropy of fluorescently labeled RNA poly(A) 50-mer upon binding to eIF4GI WT, S61A, or S61Y mutant proteins. eIF4GI protein lacking the N-terminal RNA binding domain (aa 1–82) was included as a negative control (Cont.).

antibodies showed decreased signals of PABP in the mutant cell lines. Treatment with TMG increased the amounts of PABP during pull-down in the parental cells, but had no obvious effect in the S61A knock-in cells (Fig. 5*B*). These results are consistent with the data obtained in 293T cells. Next, we investigated whether eIF4GI O-GlcNAcylation affected nascent protein synthesis. Metabolic labeling experiments with HPG consistently showed that the mutant cells exhibited a significantly lower rate of protein synthesis compared with the parental cells (Fig. 5*C*). In agreement with these results, the mutant cells also displayed lower cell proliferation in vitro and reduced ability to form colonies in the soft agar colony formation assay (Fig. 5 *D* and *E*). Thus, these results demonstrate that O-GlcNAcylation of eIF4GI positively regulates protein synthesis and cell proliferation.

Discussion

Protein synthesis is a tightly regulated process and subjected to various modes of regulation. Aberrant activity of protein synthesis has been shown to contribute to various diseases including cancer. Protein synthesis is primarily regulated at the stage of translation initiation, in which the assembly of a functional eIF4F complex is one of the rate-limiting steps. The eIF4F is regulated in cells through different mechanisms, including transcriptional control of MYC, intrinsic protein–protein interactions exerted by 4EBPs and PDCD4, and phosphorylation of the eIF4E subunit. Positioned downstream of well-established signaling pathways (e.g., PI3K/AKT/mTOR, Ras/Erk, and MYC), eIF4F serves as a key molecular mechanism linking growth factor signaling pathways with protein synthesis during cell growth and proliferation

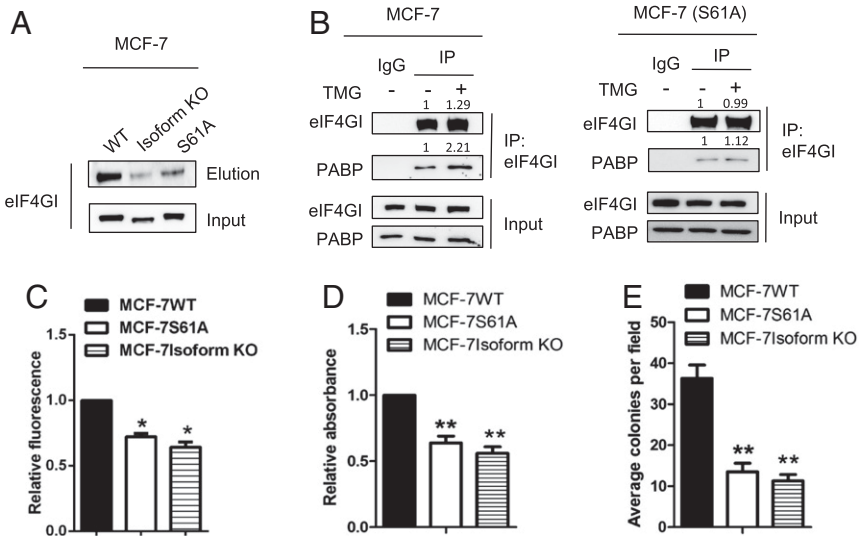

Fig. 5. O-GlcNAcylation of eIF4GI positively regulates protein synthesis and cell proliferation. (*A*) Significant decrease of eIF4GI glycosylation in eIF4GI S61A knock-in and isoform knockout (KO) MCF-7 cells, compared with the parental cells. As input, 5% of total protein was loaded as input. (*B*) The interaction between eIF4GI and PABP is increased in MCF-7 parental cells but not in MCF-7 (eIF4GI S61A knock-in) cells upon TMG treatment. Immunoprecipitation was performed using an eIF4GI antibody, and the eluent immunoblotted with a PABP antibody. Quantification of protein levels was indicated. As input, 5% of total protein was loaded. (*C*–*E*) Depletion of eIF4GI glycosylation in MCF-7 cells reduces nascent protein synthesis (*C*), cell proliferation (*D*), and soft agar colony formation (*E*). Error bars denote SEM. Statistical analysis was performed by Student's *t* test (*$P < 0.05$, **$P < 0.01$).

(40, 41). Despite the critical role of eIF4F in protein synthesis and cellular transformation, the understanding how eIF4F assembly/activity is differentially regulated in cells is far from complete. In this study, we identify O-GlcNAcylation as a mechanism for regulating eIF4F assembly and activity. We show that OGT associates with eIF4F, and directly modifies subunits eIF4A and eIF4G to modulate protein–protein interactions and the helicase activity of eIF4A. The site-specific glycosylation of eIF4A and eIF4G is shown to influence protein translation both in vitro and in vivo. Thus, our results add a dimension of complexity to the translational control of cellular proteins.

Cellular eIF4AI is the most abundant initiation factor and exists as two forms—free cytosolic protein and part of the eIF4F complex, with the majority being the free form. Even though free eIF4A proteins may not directly participate in translation initiation, studies have shown that they can exchange and incorporate into eIF4F (17, 28). How does glycosylation of eIF4A exert the inhibitory effect on protein translation? Firstly, our results show that glycosylation of eIF4A suppresses the helicase activity, an essential enzymatic activity for efficient translation initiation. Secondly, glycosylation of eIF4A at its C-terminal domain reduces the interaction with eIF4G, and possibly destabilizes the formation of a functional eIF4F. Glycosylated eIF4A can compete with free eIF4A to incorporate into eIF4F, as addition of the S322/S323Y mutant or glycosylated eIF4A in the translation system in the presence of WT eIF4A caused substantial translation inhibition (*SI Appendix*, Fig. S7). OGT is physically associated with eIF4F, and readily directs O-GlcNAcylation to eIF4A in the complex. The eIF4A in the complex is much less abundant than free eIF4A, and thus, a better target for inhibition of translation initiation. To support this, we pulled down eIF4F using m^7GDP beads and compared the O-GlcNAcylation level between the two forms of eIF4A. We showed that eIF4A in the complex displayed more than twofold higher level of glycosylation compared with free eIF4A (Fig. 1*C*). In addition, when we used a cleavable cross-linker (sulfo-NHS-SS-diazirine) to capture the transient and weak interactions in cells and pulled down eIF4F with m^7GDP, we found that glycosylation level of eIF4A was even higher compared with the samples without capture, suggesting that glycosylated eIF4A is loosely bound and tends to dissociate from the complex (*SI Appendix*, Fig. S12). Thirdly, even though the basal level of glycosylation on eIF4A in cells is about 15%, the glycosylation level can reach more than 60% upon cellular treatments, suggesting that eIF4A glycosylation is highly dynamic and responsive to environmental stimuli. This is particularly important given the various adaptations of protein synthesis in response to many different stresses and physiological conditions. Glycosylation may serve as a mechanism to fine-tune protein synthesis in cells.

Increasing evidence has demonstrated the pivotal role of O-GlcNAcylation in regulating a diverse set of proteins that function in transcription, insulin signaling, and cellular metabolism (42–44). Site-specific O-GlcNAcylation has been shown to govern the biological functions of the corresponding protein substrates (20, 45). In our study, O-GlcNAcylation of eIF4A on Ser322/323 disrupted the assembly of the eIF4F complex, inhibited its helicase activity, and led to impaired protein synthesis. In contrast, O-GlcNAcylation of eIF4G on Ser61 promoted the assembly of mRNP by enhancing the interaction with PABP and poly(A)-mRNA, thus positively regulating protein synthesis. It is quite unexpected and yet intriguing that O-GlcNAcylation plays a seemingly opposing role in regulating eIF4A and eIF4G functions. Based on our experimental observations, it appears that cancer cells selectively down-regulate eIF4A glycosylation but up-regulate eIF4G glycosylation. This differential glycosylation pattern was observed in both cell lines and tissue samples, suggesting a complex regulation of protein synthesis in vivo. We also demonstrate that during cell cycle progression, the glycosylation pattern between eIF4A and eIF4G displays an opposite trend (*SI Appendix*, Fig. S13). After m^7GDP beads pull-down, the result showed that glycosylation level of eIF4A is the highest at the S phase, and the lowest at the G2M/G1 phase. In contrast, eIF4G glycosylation level is the lowest at the S phase, and the highest at the G2M/G1 phase (*SI Appendix*, Fig. S13 *B* and *C*). Furthermore, the trend of eIF4A glycosylation was less pronounced when the whole cell lysate was directly analyzed (without m^7GDP beads pull-down), suggesting that the differential glycosylation is regulated at the level of eIF4F complex.

As OGT is the sole enzyme responsible for glycosylation of both eIF4A and eIF4G in cells, another intriguing question is, how would OGT achieve differential targeting and glycosylation of these two proteins within the same complex? Different mechanisms have been proposed to understand the activity regulation and substrate specificity of OGT, which is a topic of active research in recent years (46, 47). OGT activity is regulated by various factors, including transcription, posttranslational modifications, and sugar nucleotide (UDP-GlcNAc) concentration (48, 49). OGT substrate specificity has been proposed to occur through protein–protein interactions via its N-terminal tetratricopeptide domains (50). Given the complex regulation of OGT in cells, it is not surprising that OGT expression level or activity did not always agree with the glycosylation levels of individual proteins even within the same complex. It is also worth noting that O-GlcNAcylation can occur at different rates even at different sites within the same protein. For example, O-GlcNAcylation of CREB is only induced at Ser40 in response to neuronal activity; yet there are other sites in the protein that are basally glycosylated (51). As an extension of this study, it would be intriguing to investigate the molecular mechanism by which OGT differentially targets and glycosylates eIF4A and eIF4G under certain growth conditions or stresses.

Materials and Methods

Cell Culture and Reagents. Cell lines 293T, IOSE80, A2780, OVCAR-8, OVCAR-10, SKOV-3, GES-1, MGC803, KATO3, HGC27, MCF7, MCF10A, MDA-MB-231, LO2, HepG2, and Hep3B were all obtained from American Type Culture Collection (ATCC) and cultured according to ATCC protocols. Among them, IOSE80, GES-1, MCF10A, and LO2 are considered as noncancerous epithelia cells derived from ovarian, stomach, breast, and liver tissues, respectively. Antibodies used in this study were obtained from the following sources: anti-O-GlcNAc antibody (RL2, clone 18B10.C7, 1:1,000; Thermo Scientific), anti-eIF4AI antibody (1:1,000; Abcam), anti-eIF4B antibody (clone EP2299Y, 1:1,000; Abcam), anti-eIF4E antibody (clone Y448, 1:500; Abcam), anti-PDCD4 antibody (1:650; Sigma-Aldrich), anti-eIF4GI antibody (clone D6A6, 1:1,000; Cell Signaling Technology), anti-PABP1 antibody (1:1,000; Sigma-Aldrich), anti-Flag antibody (clone M2, 1:5,000; Sigma-Aldrich), anti-Myc antibody (1:5,000; Abmart), anti-GAPDH antibody (clone G6; Santa Cruz Biotechnology). Procedures related to human subjects were approved by the Ethic Committee of Zhejiang Cancer Hospital. The informed consent was obtained for each patient.

Chemoenzymatic Labeling and Biotinylation of O-GlcNAcylated Proteins. Cell lysate (500 μg) was labeled according to the Click-iT O-GlcNAc Enzymatic Labeling System protocol (Invitrogen), and conjugated with an alkyne–biotin compound as per the Click-iT Protein Analysis Detection Kit protocol (Invitrogen). Control experiments were carried out in parallel in the absence of the labeling enzyme GalT or UDP-GalNAz. Biotinylated lysates were precipitated using methanol and chloroform, and resolubilized in 1% SDS, and neutralized with an equal volume of neutralization buffer (6% Nonidet P-40, 100 mM Na_2HPO_4, 150 mM NaCl). Lysates were then incubated with streptavidin resin (Pierce) with end-to-end rotation at 4 °C overnight. Resins were then washed five times with 1 mL of low-salt buffer (100 mM Na_2HPO_4, 150 mM NaCl, 0.1% SDS, 1% Triton X-100, 0.5% sodium deoxycholate) and five times with 1 mL of high-salt buffer (100 mM Na_2HPO_4, 500 mM NaCl, 0.2% Triton X-100). Biotinylated proteins were eluted by boiling the resin in 50 mM Tris·HCl pH 6.8, 2.5% SDS, 100 mM DTT, 10% glycerol, and 20 mM biotin for 10 min. Western blotting analysis was carried out with indicated antibodies.

Statistical Analysis. *P* values were calculated from Student's paired *t* test when comparing within groups and from Student's unpaired *t* test when comparing between groups. For those analyses where more than one *t* test was applied to the same dataset, statistical analysis was performed by one-way analysis of variance and Bonferroni comparison posttest. Bars in graphs indicate mean ± SEM.

All other experimental methods are provided in *SI Appendix*.

ACKNOWLEDGMENTS. This work was supported by the National Science Foundation of China (Grants 91753125, 31270865, 31322019, and 31570804), the National Key Research and Development Program of China (2016YFA0100303), the National Science Foundation of Zhejiang Province (LR15C050001), and the National Institutes of Health [R01 AG060540-13 (to L.C.H.-W.)]. The tissue samples were supplied by Zhejiang Cancer Hospital Biospecimen Repository and the National Human Genetic Resources Sharing Service Platform (Grant 2005DKA21300).

1. Kong J, Lasko P (2012) Translational control in cellular and developmental processes. *Nat Rev Genet* 13:383–394.
2. Hinnebusch AG (2014) The scanning mechanism of eukaryotic translation initiation. *Annu Rev Biochem* 83:779–812.
3. Bhat M, et al. (2015) Targeting the translation machinery in cancer. *Nat Rev Drug Discov* 14:261–278.
4. De Benedetti A, Graff JR (2004) eIF-4E expression and its role in malignancies and metastases. *Oncogene* 23:3189–3199.
5. Richter JD, Sonenberg N (2005) Regulation of cap-dependent translation by eIF4E inhibitory proteins. *Nature* 433:477–480.
6. Raught B, et al. (2000) Serum-stimulated, rapamycin-sensitive phosphorylation sites in the eukaryotic translation initiation factor 4GI. *EMBO J* 19:434–444.
7. Liberman N, et al. (2015) DAP5 associates with eIF2β and eIF4AI to promote Internal Ribosome Entry Site driven translation. *Nucleic Acids Res* 43:3764–3775.
8. Chu J, et al. (2016) CRISPR-mediated drug-target validation reveals selective pharmacological inhibition of the RNA helicase, eIF4A. *Cell Rep* 15:2340–2347.
9. Boussemart L, et al. (2014) eIF4F is a nexus of resistance to anti-BRAF and anti-MEK cancer therapies. *Nature* 513:105–109.
10. Comtesse N, et al. (2007) Frequent overexpression of the genes FXR1, CLAPM1 and EIF4G located on amplicon 3q26-27 in squamous cell carcinoma of the lung. *Int J Cancer* 120:2538–2544.
11. Graff JR, et al. (2009) eIF4E activation is commonly elevated in advanced human prostate cancers and significantly related to reduced patient survival. *Cancer Res* 69: 3866–3873.
12. Silvera D, et al. (2009) Essential role for eIF4GI overexpression in the pathogenesis of inflammatory breast cancer. *Nat Cell Biol* 11:903–908.
13. Wang XL, Cai HP, Ge JH, Su XF (2012) Detection of eukaryotic translation initiation factor 4E and its clinical significance in hepatocellular carcinoma. *World J Gastroenterol* 18:2540–2544.
14. Haghighat A, Mader S, Pause A, Sonenberg N (1995) Repression of cap-dependent translation by 4E-binding protein 1: Competition with p220 for binding to eukaryotic initiation factor-4E. *EMBO J* 14:5701–5709.
15. Suzuki C, et al. (2008) PDCD4 inhibits translation initiation by binding to eIF4A using both its MA3 domains. *Proc Natl Acad Sci USA* 105:3274–3279.
16. Robichaud N, et al. (2018) Translational control in the tumor microenvironment promotes lung metastasis: Phosphorylation of eIF4E in neutrophils. *Proc Natl Acad Sci USA* 115:E2202–E2209.
17. Lee T, Pelletier J (2012) Eukaryotic initiation factor 4F: A vulnerability of tumor cells. *Future Med Chem* 4:19–31.
18. Hart GW, Housley MP, Slawson C (2007) Cycling of O-linked beta-N-acetylglucosamine on nucleocytoplasmic proteins. *Nature* 446:1017–1022.
19. Rexach JE, Clark PM, Hsieh-Wilson LC (2008) Chemical approaches to understanding O-GlcNAc glycosylation in the brain. *Nat Chem Biol* 4:97–106.
20. Rao X, et al. (2015) O-GlcNAcylation of G6PD promotes the pentose phosphate pathway and tumor growth. *Nat Commun* 6:8468.
21. Zeidan Q, Wang Z, De Maio A, Hart GW (2010) O-GlcNAc cycling enzymes associate with the translational machinery and modify core ribosomal proteins. *Mol Biol Cell* 21:1922–1936.
22. Duan F, et al. (2018) O-GlcNAcylation of RACK1 promotes hepatocellular carcinogenesis. *J Hepatol* 68:1191–1202.
23. Clark PM, et al. (2008) Direct in-gel fluorescence detection and cellular imaging of O-GlcNAc-modified proteins. *J Am Chem Soc* 130:11576–11577.
24. Datta B, Ray MK, Chakrabarti D, Wylie DE, Gupta NK (1989) Glycosylation of eukaryotic peptide chain initiation factor 2 (eIF-2)-associated 67-kDa polypeptide (p67) and its possible role in the inhibition of eIF-2 kinase-catalyzed phosphorylation of the eIF-2 alpha-subunit. *J Biol Chem* 264:20620–20624.
25. Datta R, Choudhury P, Ghosh A, Datta B (2003) A glycosylation site, 60SGTS63, of p67 is required for its ability to regulate the phosphorylation and activity of eukaryotic initiation factor 2alpha. *Biochemistry* 42:5453–5460.
26. Sonenberg N, Rupprecht KM, Hecht SM, Shatkin AJ (1979) Eukaryotic mRNA cap binding protein: Purification by affinity chromatography on sepharose-coupled m7GDP. *Proc Natl Acad Sci USA* 76:4345–4349.
27. Khidekel N, et al. (2007) Probing the dynamics of O-GlcNAc glycosylation in the brain using quantitative proteomics. *Nat Chem Biol* 3:339–348.
28. Rozovsky N, Butterworth AC, Moore MJ (2008) Interactions between eIF4AI and its accessory factors eIF4B and eIF4H. *RNA* 14:2136–2148.
29. Imataka H, Gradi A, Sonenberg N (1998) A newly identified N-terminal amino acid sequence of human eIF4G binds poly(A)-binding protein and functions in poly(A)-dependent translation. *EMBO J* 17:7480–7489.
30. Lu WT, Wilczynska A, Smith E, Bushell M (2014) The diverse roles of the eIF4A family: You are the company you keep. *Biochem Soc Trans* 42:166–172.
31. Galicia-Vázquez G, Cencic R, Robert F, Agenor AQ, Pelletier J (2012) A cellular response linking eIF4AI activity to eIF4AII transcription. *RNA* 18:1373–1384.
32. Schütz P, et al. (2010) Comparative structural analysis of human DEAD-box RNA helicases. *PLoS One* 5:e12791.
33. Oberer M, Marintchev A, Wagner G (2005) Structural basis for the enhancement of eIF4A helicase activity by eIF4G. *Genes Dev* 19:2212–2223.

34. Wang S, et al. (2012) Extensive crosstalk between O-GlcNAcylation and phosphorylation regulates Akt signaling. *PLoS One* 7:e37427.
35. Ngo JT, Tirrell DA (2011) Noncanonical amino acids in the interrogation of cellular protein synthesis. *Acc Chem Res* 44:677–685.
36. Feoktistova K, Tuvshintogs E, Do A, Fraser CS (2013) Human eIF4E promotes mRNA restructuring by stimulating eIF4A helicase activity. *Proc Natl Acad Sci USA* 110: 13339–13344.
37. Park EH, et al. (2011) Multiple elements in the eIF4G1 N-terminus promote assembly of eIF4G1•PABP mRNPs in vivo. *EMBO J* 30:302–316.
38. McKinney C, Perez C, Mohr I (2012) Poly(A) binding protein abundance regulates eukaryotic translation initiation factor 4F assembly in human cytomegalovirus-infected cells. *Proc Natl Acad Sci USA* 109:5627–5632.
39. Cheng S, Gallie DR (2007) eIF4G, eIFiso4G, and eIF4B bind the poly(A)-binding protein through overlapping sites within the RNA recognition motif domains. *J Biol Chem* 282:25247–25258.
40. Hoeffer CA, et al. (2013) Multiple components of eIF4F are required for protein synthesis-dependent hippocampal long-term potentiation. *J Neurophysiol* 109: 68–76.
41. Nasr Z, Robert F, Porco JA, Jr, Muller WJ, Pelletier J (2013) eIF4F suppression in breast cancer affects maintenance and progression. *Oncogene* 32:861–871.
42. Ferrer CM, et al. (2014) O-GlcNAcylation regulates cancer metabolism and survival stress signaling via regulation of the HIF-1 pathway. *Mol Cell* 54:820–831.
43. Jahangir Z, Ahmad W, Shabbiri K (2014) Alternate phosphorylation/O-GlcNAc modification on human insulin IRSs: A road towards impaired insulin signaling in Alzheimer and diabetes. *Adv Bioinformatics* 2014:324753.
44. Wollaston-Hayden EE, et al. (2015) Global O-GlcNAc levels modulate transcription of the adipocyte secretome during chronic insulin resistance. *Front Endocrinol (Lausanne)* 5:223.
45. Yi W, et al. (2012) Phosphofructokinase 1 glycosylation regulates cell growth and metabolism. *Science* 337:975–980.
46. Ma X, et al. (2013) Substrate specificity provides insights into the sugar donor recognition mechanism of O-GlcNAc transferase (OGT). *PLoS One* 8:e63452.
47. Aquino-Gil M, Pierce A, Perez-Cervera Y, Zenteno E, Lefebvre T (2017) OGT: A short overview of an enzyme standing out from usual glycosyltransferases. *Biochem Soc Trans* 45:365–370.
48. Roos MD, Hanover JA (2000) Structure of O-linked GlcNAc transferase: Mediator of glycan-dependent signaling. *Biochem Biophys Res Commun* 271:275–280.
49. Kapuria V, et al. (2016) Proteolysis of HCF-1 by Ser/Thr glycosylation-incompetent O-GlcNAc transferase:UDP-GlcNAc complexes. *Genes Dev* 30:960–972.
50. Levine ZG, et al. (2018) O-GlcNAc transferase recognizes protein substrates using an asparagine ladder in the tetratricopeptide repeat (TPR) superhelix. *J Am Chem Soc* 140:3510–3513.
51. Rexach JE, et al. (2012) Dynamic O-GlcNAc modification regulates CREB-mediated gene expression and memory formation. *Nat Chem Biol* 8:253–261.